

RSC Advances



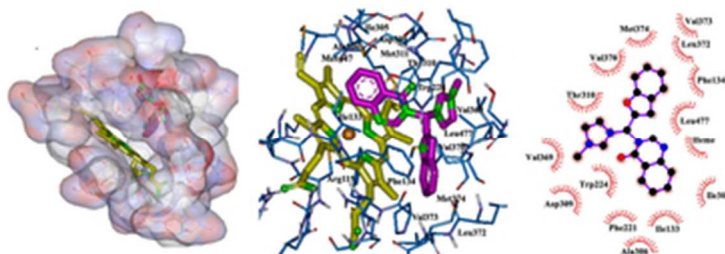
This is an *Accepted Manuscript*, which has been through the Royal Society of Chemistry peer review process and has been accepted for publication.

Accepted Manuscripts are published online shortly after acceptance, before technical editing, formatting and proof reading. Using this free service, authors can make their results available to the community, in citable form, before we publish the edited article. This *Accepted Manuscript* will be replaced by the edited, formatted and paginated article as soon as this is available.

You can find more information about *Accepted Manuscripts* in the [Information for Authors](#).

Please note that technical editing may introduce minor changes to the text and/or graphics, which may alter content. The journal's standard [Terms & Conditions](#) and the [Ethical guidelines](#) still apply. In no event shall the Royal Society of Chemistry be held responsible for any errors or omissions in this *Accepted Manuscript* or any consequences arising from the use of any information it contains.

QM/MM and docking methods was used for designing novel hybrids aromatase inhibitors incorporating benzofuran, imidazole and quinazolinone moieties



Graphical and Textual Abstract
16x8mm (600 x 600 DPI)

Design of novel potential aromatase inhibitors via hybrid pharmacophore approach: docking improvement by QM/MM method

Ghadamali Khodarahmi*¹, Parvin Asadi*¹, Hossein Farrokhpour*², Farshid Hassanzadeh¹ and Mohammad Dinari²

¹*Department of Medicinal Chemistry, School of Pharmacy and Pharmaceutical Sciences, Isfahan University of Medical Sciences, Isfahan, 81746-73461, I.R.Iran*

E-mail: khodarahmi@pharm.mui.ac.ir (G. Khodarahmi); E-mail: asadi@pharm.mui.ac.ir (P. Asadi)

²*Department of Chemistry, Isfahan University of Technology, Isfahan, 84156-83111, I.R. Iran, E-mail:h-farrokh@cc.iut.ac.ir (H. Farrokhpour)*

Abstract

Considering potent cytotoxic activities of hybrid benzofuran-imidazolium and quinazolinone derivatives on breast cancer cell line (MCF-7), novel hybrid derivatives incorporating benzofuran, imidazole and quinazolinone pharmacophores were designed by molecular hybridization approach. Since aromatase is highly expressed in MCF-7 cell line, we tried to put these pharmacophores together in such a way to arrange themselves in a symmetrical shape, similar to aromatase inhibitors. Subsequently, the binding of these novel hybrid compounds to aromatase have been investigated in a docking procedure applying a combined quantum mechanical/molecular mechanical (QM/MM) method. The QM/MM calculation was performed on the reference structures, to obtain atomic charges on the ligand atoms. The results indicated that hybrid compounds adopted properly within the aromatase binding site, suggesting that they could be potential inhibitors of aromatase. These novel designed compounds engage in hydrophobic and H bond interactions with the aromatase binding site, which are in agreement with the basic physicochemical features of known aromatase inhibitors. To obtain more accurate results for the binding energies of ligands, the structures of ligands with the best interaction energy, obtained from docking study, were re-optimized by three-layer ONIOM method (QM:QM:MM) in which the binding pocket of the enzyme was considered as a medium-level. The results demonstrated that when the optimized geometrical structures were subjected for re-docking, better interaction energy was obtained which strengthen the ability of these compounds as potential inhibitors of aromatase.

Keywords: QM/MM Docking; Pharmacophore hybridization; Benzofuran; Imidazole; Quinazolinone

1. Introduction

Application of informatics to the discovery, design and optimization of biologically active compounds which refers as computer-aided drug design (CADD) have emerged during the last decades as an important tool to help and complement experimental information. This is because, computer simulations allow a systematic and economical tool to draw biologically relevant conclusions and also propose new hypothesis based mainly on computer generated data. A large number of techniques are available for modeling of phenomena which are differing both in accuracy and speed.¹⁻³

One of the computationally inexpensive methods for predicting if and how a ligand will bind to a protein binding pocket, followed by an estimation of how strong is the ligand binding affinity, is molecular docking. This aims to achieve relative orientation of protein and ligand such that the free energy of the overall system is minimized. Given the biological and pharmaceutical significance of molecular docking, considerable efforts have been directed towards spiriting use of this method.⁴⁻⁶ In earliest docking approaches, both the ligand and the protein were treated as rigid bodies, while later semi-flexible docking was use in which the ligand is treated flexibly by allowing bonds to rotate.^{7,8} Although molecular docking simulation of proteins is a fast and inexpensive method for descriptions of the ligand-protein interactions, but poses some difficulties.⁵ Two of the most important limitations of conventional docking are assuming non protein flexibility upon ligand binding and using force field based fixed dielectric charges for both protein and ligand atoms and therefore false positives and/or false negatives in the energetic quantification of protein-ligand binding⁹. For the first problem, it should be mentioned that flexible protein docking methods, which treat the protein in a flexible manner, require high computational costs.¹⁰ About latter, it was shown that assuming fixed dielectric charges for both protein and ligand atoms lead to low accuracy in protein-ligand docking results.¹¹ Therefore, to increase accuracy in docking result, it is reasonable to expend additional effort to improve the quality of the charge.

Although, comprehensive study of polarization and charge transfer required quantum mechanical method but its use in biological models needs sophisticated computing systems.^{12,13} To limit the computational complexity, combined quantum mechanical and molecular mechanical (QM/MM) methods as an economical approach have been developed in which small portion of the protein-ligand system treated in QM detail.¹⁴⁻¹⁸ It was shown that by using an *ab initio* quantum chemical approach via QM/MM methods, a better assumption of the ligand charges, which take polarization into account, was obtained. Therefore this method could be used as a promising start towards the development of more accurate docking methods for lead optimization applications.¹¹

Molecular hybridization as a rational approach for drug design has attracted much attention by researchers to discover new chemical entities with a potential to afford some promising drugs of the future.^{19,20} In this method, active compounds and/or pharmacophoric units which recognized and derived from known bioactive molecules are fused to each other directly or with spacer. This method has been employed to develop new anticancer, anti-Alzheimer, and antimalarial agents.²¹⁻²³

Imidazole as one of the most important pharmacophores in medical chemistry has a critical role especially in antifungal, anti-bacterial, anti cancer and sedative drugs.²⁴ Its biocompatibility provides a scaffold for preparation of different derivatives to afford new bioactive compounds.²⁴ It has also been reported that imidazolium salts showed potent cytotoxic activities on different cancerous cell lines.²⁵⁻²⁷ For example, bezofuran-imidazolium hybrid compounds (1, 2) have good cytotoxic activity on MCF-7 cell line (**Scheme 1**).^{26,27} Quinazolinone is another pharmacophore which has been explored for developing pharmaceutically important molecules. Its derivatives have drawn considerable attention due to their profound chemotherapeutic properties including anticancer, antiinflammatory, anticonvulsant, and antiduritic activities.^{28,29}

Cytochrome P450 as a family of isozymes containing heme cofactor, are responsible for many critical enzymatic reactions in living systems. They are, in general, the terminal oxidase enzymes in electron transfer chains.³⁰⁻³³ Cytochrome P450 19A1, commonly known as aromatase is an enzyme of the cytochrome P450 superfamily that catalyzes the final and rate-limiting step of the conversion of androgens, testosterone and androstenedione, into estrogens, estradiol and estrone, respectively. It is comprised of a polypeptide chain of 503 amino-acid residues and a prosthetic heme group at its active site. An androgen-specific cleft consisting of hydrophobic and polar residues is situated within the confinement of the aromatase binding site. Such cleft is specific for androstenedione binding to catalyze androgen to estrogen via a three-step process. Each step requires one mol of O₂, one mol of NADPH and NADPH cytochrome reductase. This reaction converts androstenedione, testosterone and 16 α -hydroxytestosterone to estrone, 17 β -estradiol and 17 β ,16 α - estriol, respectively. The two initial steps are the typical C₁₉-methyl hydroxylation, while aromatization of the steroid A-ring is catalyzed at the final step.³⁴ To block estrogen production, it is necessary to inhibit the enzyme through the use of aromatase inhibitors.³⁵

According to the previous studies, bezofuran-imidazole analogs as well as quinazolinone derivatives (**2**) have good cytotoxic effect on MCF-7 cell line (**Scheme 1**).^{26,27,36,37} therefore selecting quinazolinone and bezofuran-imidazole moieties together as potential cytotoxic agent on this cell line would be logical. On the other hand benzofuran was used in the structure of some potent aromatase inhibitors.^{38,39,40} For example, Whomsly et al.³⁸ identified substituted 1-[(benzofuran-2-yl)-phenylmethyl]-imidazoles (**3**) as a class of potent aromatase inhibitor with in vitro IC₅₀ values < 10 nM which is 80-1000 times of the inhibitory activity of aminoglutethimide (**Scheme 1**). Since aromatase is overexpressed in MCF-7 cell line, we want to rationally design novel structure that incorporates these moieties into a single molecular scaffold which could act as an aromatase inhibitor. According to

previous study ⁴¹, besides the physicochemical properties of the inhibitor, molecular shape is expected to be extremely important to the access and fit within the active site of the aromatase. Most aromatase inhibitors used to build the common features model have a similar shape that is expected to be complementary to the volume of the aromatase active site. For example letrozole (**Scheme 1**) a quite rigid third generation inhibitor of aromatase has a high degree of symmetry. To obtain a final symmetrical shape, which consists of three pharmacophores, best arrangement is to put each of the pharmacophores on triangle vertices. As the basic physicochemical features of known aromatase inhibitors are high degree of hydrophobicity and the potential to establish hydrogen bonds, ^{42,43} it is expected that this structure with heterocyclic ring provide the desired hydrophobicity. On the other hand, hetero atoms in the ring and substitutions located on the structure provide the hydrogen bond potential for this structure.

partial charges of the ligand were re-fitted according to the polarized active site environment of the enzyme to increase the accuracy of the docking results. Then, the structures with the best interaction energy obtained from docking study were optimized by three-layer ONIOM method and finally re-docked to 3D structure of enzyme to obtain interaction energy. The result demonstrated that these novel designed compounds have good interaction energy and could be used as potential aromatase inhibitors.

2. Experimental

2.1. Docking method

Molecular docking was performed by AutoDock4 software to elucidate the binding mode of aromatase with novel hybrid compounds.⁴⁴ The atomic coordinate of the protein was obtained from Protein Data Bank using PDB id 3EQM. The protein structure was visualized and all water molecules were eliminated from the protein structure. The structures of ligands were optimized using the PM6 semi-empirical method in Gaussian 09 quantum chemistry package. AutoDockTools was used to prepare the molecules and parameters before submitting it for docking analysis with AutoDock. For this purpose, polar hydrogen atoms were added while non-polar hydrogen atoms were merged assuming a physiological pH value of 7.0. Then, Gasteier partial atomic charges were assigned to the ligands. All rotatable bonds of ligands, defined by default of the program, were allowed to rotate during the automated docking process and then prepared protein and ligand structures were saved in the PDBQT format suitable for calculating energy grid maps. A grid box size of $60 \times 60 \times 60$ Å points with a grid spacing of 0.375 Å was considered which its center was defined as the center of the co-crystallized inhibitor. Van der Waals and the electrostatic terms were calculated by AutoDock parameter functions. The initial position, orientation and torsions of the ligand molecules were set randomly. Each docked compound was derived from 100 independent docking runs that were set to terminate after a maximum of 2.5×10^6 energy evaluations with

mutation rate of 0.02 and crossover rate of 0.8. The population size was set to use 250 randomly placed individuals. The search for low-energy binding orientations was performed by Lamarckian Genetic Algorithm using a translational step of 0.2 Å, a quaternion step of 5 Å and a torsion step of 5 Å. To conclude, the free energies of binding (ΔG_b) and inhibition constants (K_i) were calculated by AutoDock. Several clusters and binding energies were obtained for docked hybrid compounds in which the best conformers were selected according to the lower docked free energy and top-ranked cluster to perform docking analysis with AutoDock Tools and PyMOL. To evaluate the validity of the docking process, the substrate of enzyme, androstenedione, was extracted from the binding cavity and re-docked to the aromatase enzyme. According to root mean square deviation (RMSD) of 1.47 Å, orientation of the re-docked substrate was nearly identical to the X-ray crystallographic conformer which this confirmed validity of docking. Molecular docking simulations of proteins where ligand binding involves prosthetic groups like NAD or HEM (in our case the iron atom of the heme cofactor) poses a great challenge. In this study, a set of charges obtain from the work of Favia et al. calculated using DFT method considering B3LYP functional and 6-31G(d) basis set was applied for the heme cofactor and used in molecular docking.⁴⁵

2.2. QM/MM Methodology

For QM/MM calculations, we employed the Gaussian 09 quantum chemistry package.⁴⁶ “Our own N-layered integrated molecular orbital and molecular mechanic” abbreviated as ONIOM method implemented in Gaussian 09 was used for QM/MM calculations.⁴⁷ The ONIOM scheme is more general in the sense that it can combine any number of molecular orbital methods as well as molecular mechanics method and is considered as QM/MM method. This method enables different *ab initio* or semi-empirical methods to be applied to different parts of a system. The interactions between ligand and

protein are exclusively non-covalent, therefore, ligand was assumed as the QM region and the protein as the MM region. For obtaining partial atomic charge of ligand atoms in the active site of aromatase, PM6 semi-empirical method, one of the best semi-empirical methods in quantum mechanics, was used to represent the QM region (ligand) and the universal force field (UFF) was used for the MM region (aromatase). Therefore, a two layer ONIOM calculations (PM6:UFF) was used for the calculations. The partial atomic charges of the MM region were assigned using the QEq formalism.⁴⁷ The partial atomic charges of the ligands obtained through QM/MM calculations were used to increase the accuracy of docking calculations.

To more increase the accuracy of the docking results, three layer ONIOM calculations (QM:QM:MM) calculations were performed on the structures with the best interaction energy obtained from the previous docking study. For this purpose, the geometry of ligand along with the porphyrin structure of heme-iron and several residue including Met 374, Val 373, Val 370, Ile 305, Ala 306, Ile 133, Trp 224, Leu 372, Leu 477, Phe 134 and Thr 310 were optimized in the field of protein. The density functional theory (DFT) method employing B3LYP/LANL2MB/6-31G(d) basis set was used for the high-level part of system (ligand). PM6 semiempirical method was used for the medium part of system (heme-iron and the residues) and UFF was employed for the rest of protein.

3. Results and Discussion

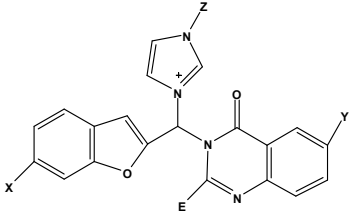
As mentioned above, the bezofuran-imidazole and quinazolinone analogs have shown good cytotoxic effect on MCF-7 cell line. In this study, by means of molecular hybridization method, novel hybrid compounds bearing imidazole, benzofuran and quinazolinones were designed as potential cytotoxic agents (scheme 1). It was expected that, if the spatial orientation of these hybrid compounds be symmetrical, similar to azol-type aromatase

inhibitors,⁴¹ they could interact with aromatase enzyme. The binding modes of these novel compounds to aromatase were investigated through docking method.

The prediction of the binding affinity in a molecular docking tool is estimated by a scoring function, which generally needs to be both fast and accurate. The electronic interaction is one of the important components of the energy model. So, assuming fixed dielectric charge for protein and ligand atoms, this is considered in docking procedure, lead to low accuracy of docking results. This problem is more important for proteins with metal ion in their active site. In fact, the presence of metal ion induces higher polarization effect and enhances restriction of docking in prediction of electronic interactions. In this study, owing to the positive charge on imidazole ring of the designed compounds and also the presence of Heme iron in the active site, polarization effects is more important in energy calculations. So, to enhance the accuracy of the results, improvement of the charge model should be considered. QM/MM methods can help to offer superior estimate of the electronic interactions. Previous studies have shown that docking program gives better results if the ligand partial charges are refitted with QM/MM.¹¹ In the present study we performed the QM/MM calculation on the reference structures, to obtain atomic charges on ligand atoms. These calculated charges are presumed to represent the reasonable accuracy for the ligand atom charges that are polarized by the surrounding atoms of the receptor molecule within the binding sites. Then, the ligands with improved charges were employed for re-docking into the aromatase enzyme. Since top-scoring pose in docking is depending to charges of the ligand atoms, these two steps were repeated until change in the charge values became insignificant. Autodock4 was used to dock the new hybrid compounds into the aromatase enzyme and record the top scoring structure. Next, QM/MM calculation was performed in which the ligand was treated via PM6 calculation as the QM level, and new atomic charges on the ligand atoms were obtain by Mulliken population analysis. Once charge values in the ligand

files were substituted with these new charge values, another autodock4 run was performed and top scoring structure was recorded again. After repeating these operations for three times, charges were almost constant which were used for final docking process. Subsequently, with selection of the best complex between ligand and protein according to its cluster and binding energy, important interactions were investigated. The free energies of binding (ΔG_b) and inhibition constants (K_i) as calculated by AutoDock are summarized in Table 1.

Table 1. Chemical structures and the changes of free binding energy (kcal/mol) during determination of more accurate charges according to protein active site obtained from single point QM/MM calculations as well as inhibition constants (K_i) of ligands after refitting the charges calculated by AutoDock.

									
No	X	Y	Z	E	cluster	Binding energy ⁽¹⁾	Binding energy ⁽²⁾	Binding energy ⁽³⁾	K_i ⁽⁴⁾
1.	H	H	Methyl	H	61	-7.77	-7.83	-7.81	2.00 μ M
2.	Cl	H	Methyl	H	60	-7.83	-7.97	-7.95	1.50 μ M
3.	Cl	Cl	Methyl	H	49	-8.21	-8.35	-8.34	632.00 nM
4.	OH	H	Methyl	H	52	-7.77	-8.80	-8.82	409.00 nM
5.	OH	Methyl	Methyl	H	50	-8.08	-8.32	-8.35	610.00 nM
6.	OH	OH	Methyl	H	73	-9.14	-9.32	-9.34	68.00 nM
7.	Methoxy	H	Methyl	H	46	-8.14	-8.30	-8.33	640.00 nM
8.	Methoxy	Br	Methyl	H	40	-7.61	-7.74	-7.73	2.29 μ M
9.	Methoxy	H	Propyl	H	32	-6.27	-6.41	-6.43	17.50 μ M
10.	Br	H	Methyl	H	34	-7.29	-7.39	-7.41	4.25 μ M

11.	OH	H	Methyl	H	74	-8.18	-8.38	-8.37	1.07 μM
12.	OH	Cl	Propyl	H	20	-7.77	-8.01	-8.07	1.20 μM
13.	Br	OH	Propyl	H	12	-6.84	-6.54	-6.57	15.00 μM
14.	Methoxy	OH	Propyl	H	16	-6.48	-6.37	-6.34	22.00 μM
15.	OH	Methoxy	Methyl	H	38	-7.92	-8.36	-8.33	639.00 μM
16.	OH	Cl	Methyl	H	54	-8.71	-8.80	-8.86	411.00 nM
17.	OH	Br	Methyl	H	48	-8.76	-8.86	-8.85	423.00 nM
18.	OH	Methoxy	Propyl	H	12	-6.80	-6.63	-6.66	17.03 μM
19.	OH	OH	Propyl	H	36	-7.12	-7.28	-7.21	4.51 μM
20.	OH	H	Propyl	H	24	-7.54	-7.09	-7.12	6.04 μM
21.	OH	Methyl	Propyl	H	8	-6.19	-6.54	-6.56	15.35 μM
22.	OH	Cl	Methyl	Thiophene	20	-6.13	-5.80	-5.83	48.81 μM
23.	OH	Br	Methyl	Thiophene	20	-6.56	-6.08	-6.10	25.00 μM
24.	OH	Methoxy	Methyl	Thiophene	36	-6.27	-5.98	-6.01	39.00 μM
25.	OH	OH	Methyl	Thiophene	42	-6.34	-7.01	-7.08	5.72 μM
26.	OH	H	Methyl	Thiophene	66	-5.65	-5.40	-5.44	106.00 μM
27.	OH	Methyl	Methyl	Thiophene	32	-5.72	-5.32	-5.35	110.00 μM
28.	OH	Cl	Propyl	Thiophene	14	-5.41	-5.31	-5.28	113.00 μM
29.	OH	Br	Propyl	Thiophene	10	-5.74	-5.31	-5.38	112.00 μM
30.	OH	Methoxy	Propyl	Thiophene	8	-5.62	-5.46	-5.50	213.00 μM
31.	Methoxy	H	Methyl	H	36	-8.09	-8.31	-8.34	825.00 nM
32.	Methoxy	Methyl	Methyl	H	50	-7.8	-8.01	-8.08	1.18 μM
33.	Methoxy	OH	Methyl	H	42	-7.92	-7.97	-8.02	1.19 μM
34.	Methoxy	Methoxy	Methyl	H	40	-8.15	-8.55	-8.56	530.00 nM
35.	Methoxy	Cl	Methyl	H	58	-7.61	-7.98	-8.03	1.19 μM
36.	Methoxy	Br	Methyl	H	54	-7.82	-8.02	-8.13	1.04 μM
37.	Methoxy	Methoxy	Propyl	H	30	-6.68	-6.34	-6.33	22.00 μM
38.	Methoxy	OH	Propyl	H	79	-6.74	-6.8	-6.79	11.40 μM
39.	Methoxy	H	Propyl	H	87	-6.17	-6.30	-6.34	9.26 μM

40.	Methoxy	Methyl	Propyl	H	10	-6.03	-5.83	-5.86	31.86 μM
41.	Methoxy	Cl	Methyl	Thiophene	41	-6.01	-5.97	-5.96	55.74 nM
42.	Methoxy	Br	Methyl	Thiophene	20	-5.78	-5.60	-5.59	70.00 μM
43.	Methoxy	Methoxy	Methyl	Thiophene	50	-6.04	-5.93	-5.91	44.60 μM
44.	Methoxy	OH	Methyl	Thiophene	36	-6.19	-6.09	-6.06	36.33 μM
45.	Methoxy	H	Methyl	Thiophene	50	-6.01	-5.97	-5.98	44.45 μM
46.	Cl	H	Methyl	H	30	-7.73	-7.88	-7.85	1.61 μM
47.	Cl	Methyl	Methyl	H	60	-8.15	-8.34	-8.36	825.00 nM
48.	Cl	OH	Methyl	H	54	-8.30	-8.44	-8.45	642.00 nM
49.	Cl	Methoxy	Methyl	H	54	-8.00	-8.65	-8.59	531.00 nM
50.	Cl	Cl	Methyl	H	62	-7.78	-8.02	-8.04	1.21 μM
51.	Cl	Br	Methyl	H	58	-7.64	-7.81	-7.79	1.69 μM
52.	Cl	Methoxy	Propyl	H	14	-5.59	-6.01	-5.93	44.58 μM
53.	Cl	OH	Propyl	H	12	-6.02	-6.21	-6.17	30.89 μM
54.	Cl	H	Propyl	H	22	-6.60	-6.13	-6.20	26.68 μM
55.	Cl	Methyl	Propyl	H	18	-6.16	-5.99	-5.95	5.68 μM
56.	Methyl	H	Methyl	H	30	-6.89	-6.97	-6.95	8.78 μM
57.	Methyl	Methyl	Methyl	H	40	-7.02	-7.62	-7.65	14.74 μM
58.	Methyl	OH	Methyl	H	16	-7.95	-8.45	-8.42	644.00 nM
59.	Methyl	Methoxy	Methyl	H	34	-7.35	-7.85	-7.81	13.69 μM
60.	Methyl	Cl	Methyl	H	30	-7.97	-8.35	-8.38	820.00 μM
61.	Methyl	Methoxy	Propyl	H	36	-5.32	-5.65	-5.62	67.00 μM
62.	Methyl	OH	Propyl	H	24	-6.24	-6.01	-6.05	38.12 μM
63.	Methyl	H	Propyl	H	52	-6.18	-6.45	-6.44	18.74 μM
64.	Methyl	Methyl	Propyl	H	58	-6.57	-6.76	-6.71	11.04 μM

(1) The first binding energy calculated with autodock

(2) The binding energy calculated after refitting charge with the values obtained from QM/MM calculation

(3) The binding energy calculated after fixed charge values

In addition to the physicochemical properties of the inhibitor, molecular shape is also expected to be extremely important for accessing and fitting within the active site of the aromatase. Docking analyses revealed that the novel hybrid compounds obtained from this investigation could fit well within the binding site cavity (Fig. 1) to form a three branched shape similar to the most third generation aromatase inhibitors⁴¹. As shown previously, high degree of hydrophobicity and the potential to establish hydrogen bonds with the aromatase enzyme are the basic physicochemical features of known aromatase inhibitors.⁴² These properties are related to the non-polar binding pocket of the enzyme which is dominated by aliphatic amino acid residues such as Met 374, Val 373, Val 370, Ile 305, Ala 306, Ile 133, Trp 224, Leu 372, Leu 477, Phe 134 and Thr 310.⁴² Newly designed compounds could well meet required hydrophobic interaction through quinazolinone, benzofuran and imidazole moieties. Examination of the best-ranked docking reveals that among the three heteroaromatic rings located in the substrate cavity, relatively quinazolinone nucleus was in close vicinity of the Heme iron. This feature reflects the binding mechanism found for this type of molecule, which explain binding through heterocyclic aromatic coordination to the heme iron of the P450 active site. However, no H-bond was predicted for N₃ of quinazolinone from the docking results. Additionally, π - π conjugate interactions are formed among Phe221, Trp224, Ile133 and phenyl ring of quinazolinone. The benzofuran ring of the hybrid compounds is found to match through hydrophobic interactions with Phe134, Val370, Leu372 and Met374. In some cases the oxygen atom of the benzofuran ring formed a hydrogen bond with Asp309 which is in close proximity to benzofuran. The imidazole ring was oriented to make hydrophobic interactions with the Trp224, Val369 and Thr310 residues. Hydrophobic interaction observed for cationic imidazole ring is interesting. The reason can be stated is that these cation isn't a simple point charge which only be involved in electrostatic interactions but it is a delocalized charge in imidazolium ring. This

delocalization lead to distribution of a positively charged on the five atom of ring such that carbon and hydrogen are still able to participate in hydrophobic interactions as seen in fig drawn from lig plot. It should be mentioned that in this scaffold, due to the presence of a positive charge on the nitrogen atom of imidazole, it seems logical to be accommodated away from the Heme iron. Also, because of the resonance effect, none of the nitrogens of imidazole could make hydrogen bonds with the residues in aromatase active site.

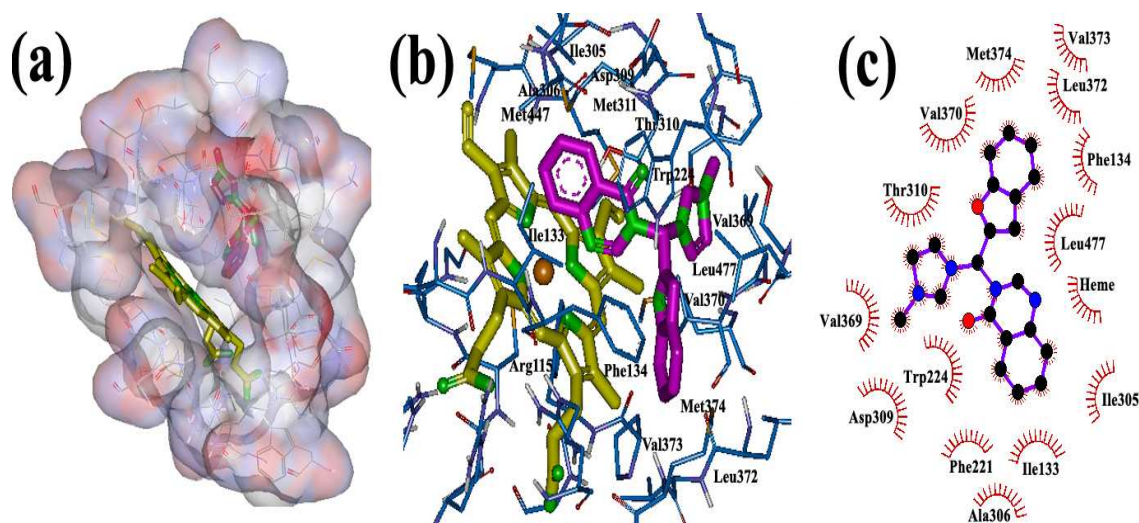


Fig. 1. The binding mode of new hybrid scaffold in active site of aromatase obtained from autodock4 (a , b) 3D structure, (c) 2D structure.

In the next step, butyl, halogen, hydroxyl and methoxy groups were appropriately substituted on the heteroaromatic rings of the designed compounds and their binding modes were investigated through docking. The new analogs share the same binding modes similar to the unsubstituted derivatives, with extra anchoring point which might cause stronger binding to aromatase active site. The main binding modes in these complexes can be described as following: Introduction of OH on the benzofuran ring caused formation of hydrogen bonds with the amino acid residue Ser 478 of aromatase (Fig. 2), while OH group on quinazolinone ring exhibited H-bond with Met374 (Fig. 3). In structure with two hydroxyl groups

substituted on both quinazolinone and benzofuran both of the mentioned H bonds are visible (Fig. 4).

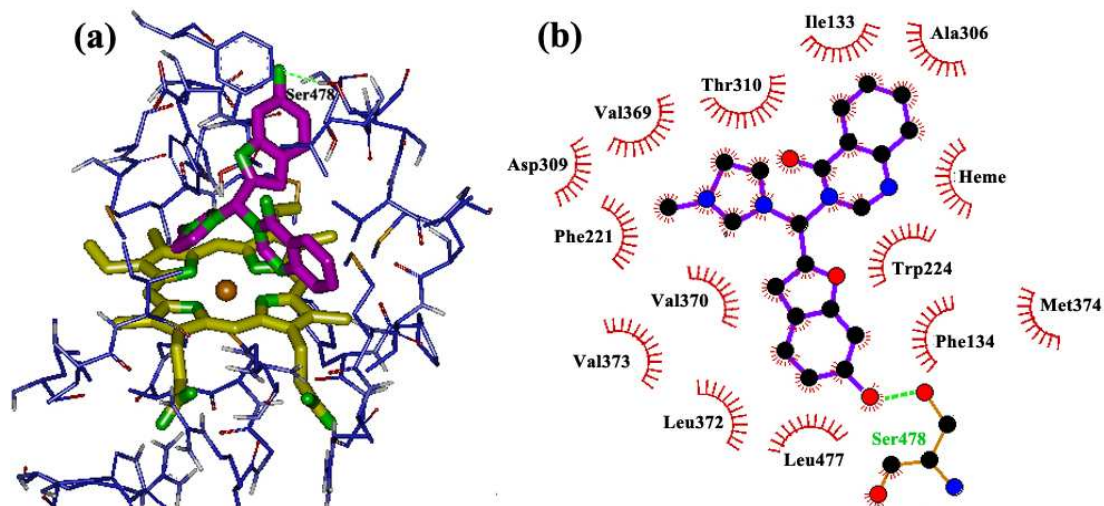


Fig. 2. Binding modes and hydrogen bonds interactions of hydroxyl group on benzofuran ring with Ser 478 in aromatase active site (a) 3D structure, (b) 2D structure

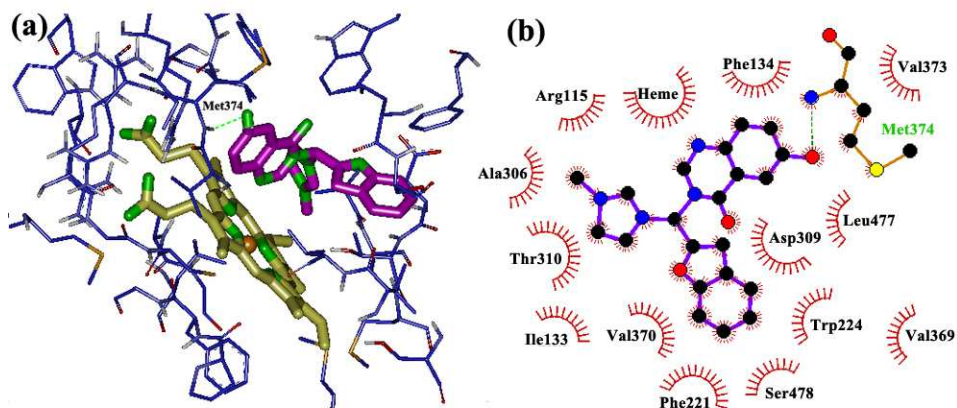


Fig. 3. Binding modes and hydrogen bonds interactions of hydroxyl group on quinazolinone ring with Met374 in aromatase active site (a) 3D structure, (b) 2D structure

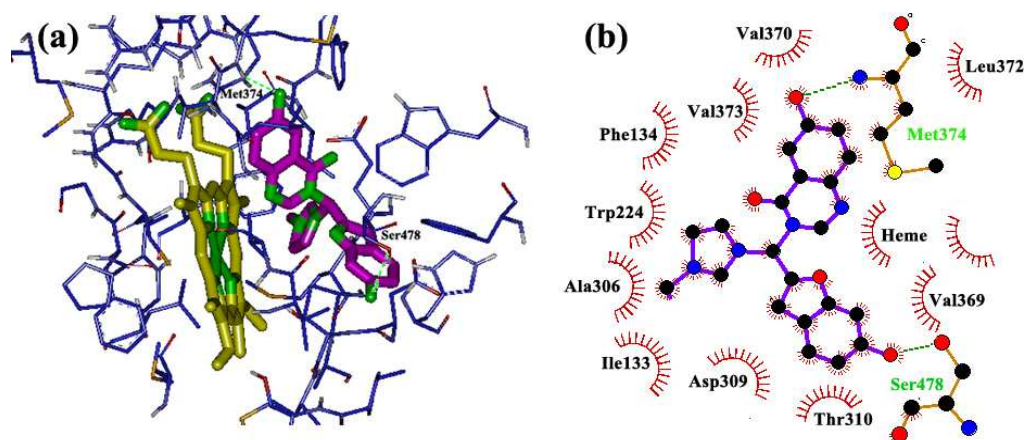


Fig. 4. Binding modes and hydrogen bonds interactions of hydroxyl group on both quinazolinone and benzofuran rings with Ser478 and Met374 in aromatase active site respectively (a) 3D structure, (b) 2D structure

Insertion of methoxy group on quinazolinone and/or benzofuran systems also caused formation of H-bond with hydrogen-bond donors in the active site of the enzyme. The methoxy group on benzofuran ring and Ser478 are in close proximity (Fig. 5) with favorable hydrogen bonding interactions while Met374 formed a hydrogen bond with the methoxy group on quinazolinone ring (Fig. 6). Additionally hydrophobic substituent such as chloro and methyl groups on quinazolinone and benzofuran ring, somewhat increase aromatase inhibition potency through increased hydrophobic interactions. Chloro and methyl substituents on quinazolinone ring stabilized by van der Waals interactions with the non polar amino acids in the active site (Ala306, Thr310, Trp224, Val370, Ile133, Phe134, Leu372 and Val373), while chloro and methyl on benzofuran ring involved in the hydrophobic interactions with the hydrophobic residues Ile133, Phe134, Leu372 and Val369. Finally, substitution of small alkyl group such as methyl on imidazolium ring make its access and accommodation to the active site easier compare to the bulkier butyl group.

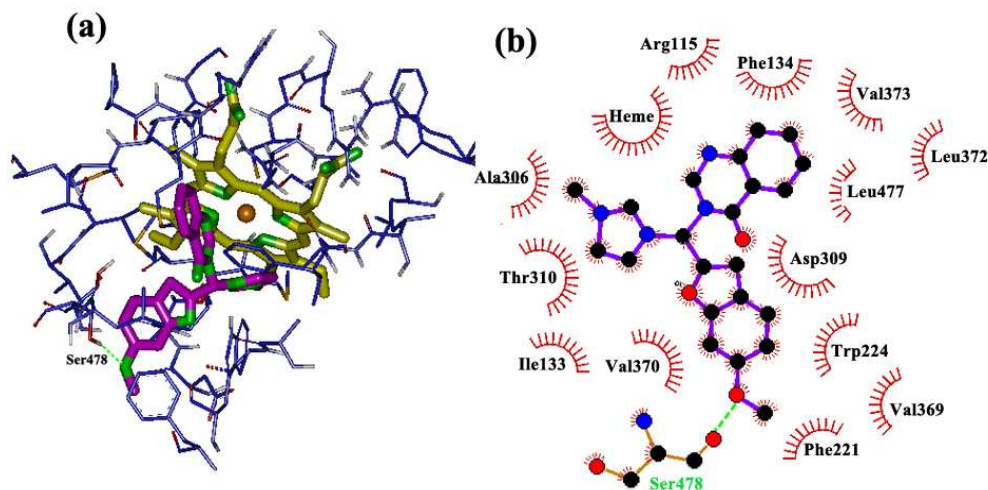


Fig. 5. Binding modes and hydrogen bonds interactions of methoxy group on benzofuran ring with Ser478 in aromatase active site **(a)** 3D structure, **(b)** 2D structure

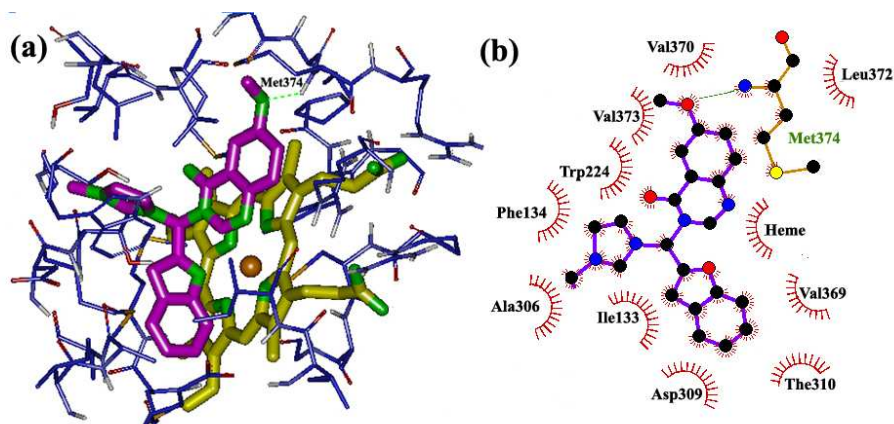


Fig. 6. Binding modes and hydrogen bonds interactions of methoxy group on quinazolinone ring with Met374 in aromatase active site **(a)** 3D structure, **(b)** 2D structure

The structures with the best Gibbs interaction energies obtained through the previous docking were re-optimized using three-layer ONIOM method. In other words, the structure of ligand along with the interacting residues and heme-iron was optimized in the electrostatic field of the rest protein which is freeze. The advantage of this method is that the ligand is optimized in the presence of protein and its structure is more reliable than before. In addition,

the geometrical structures of the residues interacting with the ligand are improved by this optimization. For the high level layer we used designed inhibitors inside the aromatase active site, for the medium level we used heme-iron and several residues from the binding pocket, including as Met 374, Val 373, Val 370, Ile 305, Ala 306, Ile 133, Trp 224, Leu 372, Leu 477, Phe 134 and Thr 310 and the remainder of the protein is treated for the low level as depicted in Fig. 7. After the geometric parameters of the molecules are fully optimized, ligands were extracted from complexes and were subjected for rigid re-docking. It means that all rotatable bonds were to be held constant and ligand charges were replaced with obtained values from QMMM calculation. The results showed that all runs extended to creation of one cluster and also the calculated ΔG s increases as much as 1-2 kcal/mol for ligands (Table 2) In early QM/MM calculation we only used the charges but in the final QM/MM calculation the same optimized ligand in protein environment was used for autodock in the same figure which showed if structure of ligand was optimized in the active sit of enzyme and then the same optimized ligand was de-docked to protein; the lower binding energy was obtained.

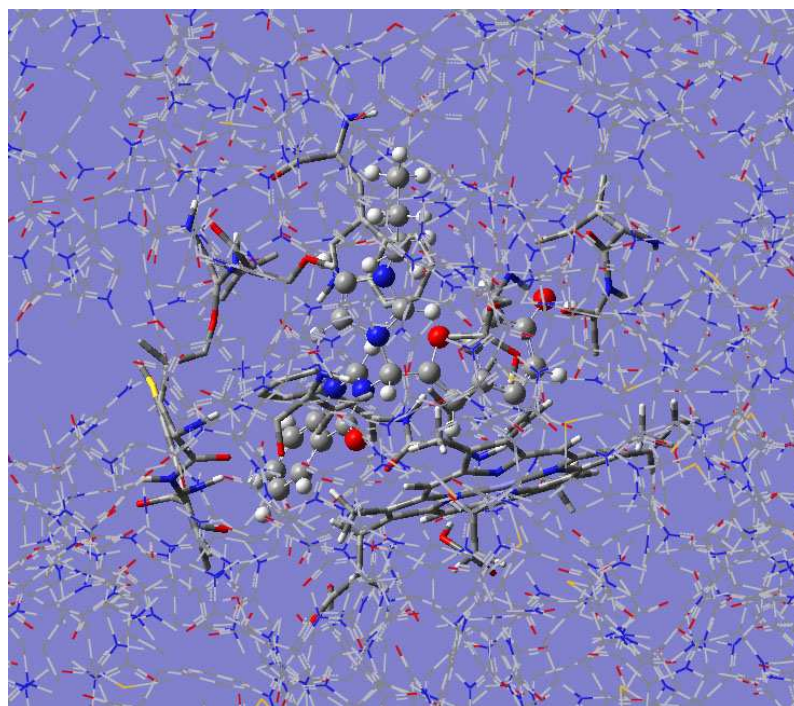


Fig. 7. Inhibitor-enzyme model used for ONIOM calculations: The ball and stick representation is used for the high (large spheres) and medium (small spheres) layer atoms and the lines are used for the low layer atoms.

Table 2. Comparison of free energies of binding (ΔG_b) in Kcal/mol and inhibition constants (K_i) calculated by AutoDock before and after optimization via three-layer ONIOM method.

NO	ΔG_b docking after refitting of ligand charge	K_i after refitting of ligand charge	RMSD	ΔG_b in rigid docking	K_i in rigid docking	RMSD
4	-8.82	409 nM	0.31	-10.11	37.00 nM	0.14
6	-9.34	68 nM	0.27	-11.47	4.39 nM	0.16
16	-8.86	411 nM	0.25	-9.94	65.00 nM	0.14
17	-8.85	423 nM	0.36	-9.75	66.00 nM	0.11
34	-8.56	530 nM	0.41	-9.95	65.00 nM	0.21
48	-8.45	642 nM	0.28	-10.81	9.69 nM	0.11
49	-8.59	531 nM	0.25	-10.41	12.44 nM	0.16
58	-8.42	644 nM	0.38	-10.23	17.00 nM	0.12

According to the above results, the designed ligands formed a three branched structures in the protein environment which accommodated well into the active site. We found that in addition of the Van der Waals interactions, hydrogen bonds are key factors for ligand-receptor interactions. Compound 6 which yielded the highest ΔG_b (-11.47) and the best performing K_i (48nM) values was assuming to be the best ligand. Since the assay method used for evaluating the anti aromatase potencies of the compounds was theoretical, the precise assessment of aromatase inhibition as the mechanism of action for these compounds needs further studies. Based on the results of the present research, synthesis and cytotoxic evaluation of the designed derivatives are undergoing in our research group.

4. Conclusions

In summary, in this study we development of novel potential aromatase inhibitors that contain substituted benzofuran, quinazolinone and imidazole rings. Docking simulation was carried out to identify interactions of these ligands with aromatase enzyme. Since polarization effects are involved in the interaction energy, QM/MM calculations was performed in which atomic charges on ligand atoms calculated with reasonable accuracy according to polarization effect by the surrounding atoms of the receptor molecule within the binding sites. Using the new set of charge values, the docking was performed again. These two steps were repeated three times until change in charge reached to a negligible value. At the end, the lowest energy structure (taking into account the charge polarization) was selected which showed that design hybrid compounds adopted properly within the aromatase binding site. On the other hand re-docking of ligands which were optimized via three-layer ONIOM method resulted in better ΔG_s , confirming the ability of these designed compounds as potential inhibitors of aromatase. According to the above results, compound 6 with $K_i= 48\text{nM}$ and $\Delta G_b= -11.47 \text{ kcal/mol}$ has the highest interaction with aromatase.

Acknowledgment

We gratefully acknowledge the financial support from the Iran National Science Foundation (INSF) with project number of 90001304 and Research Council of Isfahan University of Medical Sciences.

Notes

The authors declare no competing financial interest.

References

- 1 P.P. Kore, M.M. Mutha, RV. Antre, R.J. Oswal and S.S. Kshirsagar, *Open J Med Chem.*, 2012, **2**, 139-148

- 2 G. Sliwoski, S. Kothiwale, J. Meiler and E.W. Lowe, *Pharmacol Rev.*, 2014, **66**, 334-395
- 3 W.L. Jorgensen, *Science.*, 2004, **303**, 1813-1818
- 4 R.D. Taylor, P.J. Jewsbury and J.W. Essex, *J. Comput aided Molecul. Design.*, 2002, **16**, 151-166
- 5 S.F. Sousa, P.A. Fernandes and M.J. Ramos, *Structure, Function, and Bioinformatics.*, 2006, **65**, 15-26
- 6 P.P. Roy and K. Roy, *J Pharm Pharmacol.*, 2010, **62**, 1717-1728
- 7 R.T. Kroemer, *Curr Protein Peptide Sci.*, 2007, **8**, 312-328
- 8 D.S. Goodsell, G.M. Morris and A.J. Olson, *J Moll Recogn.*, 1996, **9**, 1-5
- 9 M. Xu and M.A. Lill, *Drug Discov Today Technol.*, 2013, **10**, 411-418
- 10 M. Totrov and R. Abagyan, *Curr Opin Struct Biol.*, 2008, **18**, 178-184
- 11 A.E. Cho, V. Guallar, B. Berne and R. Friesner, *J Comput Chem.*, 2005, **26**, 915-931
- 12 K. Raha, M.T.B. Peters, B. Wang, N. Yu, A.M. Wollacott, L.M. Westerhoff and K.M. Merz, *Today.*, 2007, **112**, 725-731
- 13 H. Liu, M. Elstner, E. Kaxiras, T. Frauenheim, J. Hermans and W. Yang, *Protein Struct Funct Genet.*, 2001, **44**, 484-489
- 14 A. Warshel, *Angew. Chem.*, 2014, **53**, 10020-10031
- 15 S. Grimme, *Wiley Interdiscip Rev Comput Mol Sci.*, 2011, 211-228
- 16 S.C.L. Kamerlin and A. Warshel, *Proteins-Structure Function and Bioinformatics*, 2010, **78**, 1339-1375
- 17 A. Warshel, *Computer Modeling of Chemical Reactions in Enzymes and Solutions*, Wiley 1997
- 18 M. Repic, R. Vianello, M. Purg, F. Duarte, P. Bauer, S. C. L. Kamerlin and J. Mavri, *PROTEINS: Struct Func Bioinform.*, 2014, **82**, 3347-3355
- 19 C. Lazar, A. Kluczyk, T. Kiyota, Y. Konishi, *J Med Chem.*, 2004, **47**, 6973-6982

- 20 R.A. Rane, V.N. Telvekar, *Med Chem Lett.*, 2010, **20**, 5681-5685
- 21 K.V. Sashidhara, A. Kumar, M. Kumar, J. Sarkar and S. Sinha, *Bioorg Med Chem Lett.*, 2010, **20**, 7205-7211
- 22 S. Rizzo, C. Riviere, L. Piazzzi, R. Stefano, B. Alessandra, S. Gobbi, M. Bartolini, V. Andrisano, F. Morroni, A. Tarozzi, J.P. Monti and A. Rampa, *J Med Chem.*, 2008, **51**, 2883-2886
- 23 F.W. Muregi and A. Ishi., *Drug Develop Res.*, 2010, **71**, 20-32
- 24 P. Molina, A. Tarraga and F. Oton, *Org Biomol Chem.*, 2012, **10**, 1711-1724
- 25 X.D. Yang, X.H. Zeng, Y.L. Zhang, C. Qing, W.J. Song, L. Li and H.B. Zhang, *Bioorg Med Chem Lett.*, 2009, **19**, 1892-1895
- 26 X.D. Yang, W.C. Wan, X.Y. Deng, Y. Li, L.J. Yang, L. Li and H.B. Zhang, *Bioorg Med Chem Lett.*, 2012, **22**, 2726-2729
- 27 W. Chen, X.Y. Deng, Y. Li, L.J. Yang, W.C. Wan, X.Q. Wang, H.B. Zhang and X.D. Yang, *Bioorg Med Chem Lett.* 2013, **23**, 4297-4302
- 28 D. Wang and F. Gao, *Chem Cent J.*, 2013, **7**, 95-110
- 29 A.S. ElAzab, M. AlOmar and A. Abdel, *Euro J Med Chem.*, 2010, **45**, 4188-4198
- 30 P.S. Pallan, C. Wang, L. Lei, F.K. Yoshimoto, R.J. Auchus, M.R. Waterman, F.P. Guengerich, and M. Egli, *J Biol Chem.*, 2015, **290**, 13128-13143
- 31 P.S. Pallan, L.D. Nagy, L. Lei, E. Gonzalez, V.M. Kramlinger, C.M. Azumaya, Z. Wawrzak, M.R. Waterman, F.P. Guengerich, M. Egli, *Biol Chem.*, 2015, **290**, 3248-3268
- 32 S. Goyal, Y. Xiao, N.A. Porter, L. Xu, and F.P. Guengerich, *J Lipid Res.*, 2014, **55**, 1933-1943
- 33 G. Chowdhury, N. Shibata, H. Yamazaki and F. Peter Guengerich, *Chem Res Toxicol.*, 2014, **27**, 147-156
- 34 J.C. Hackett, R.W. Brueggemeier, C.M. Hadad, *J Am Chem Soc.*, 2005, **127**, 5224-5237

- 35 R.W. Brueggemeier, J.C. Hackett, E.S. Diaz-Cruz, *Endocr Rev.*, 2005, **26**, 331-345
- 36 G.A. Khodarahmi, M.R. Khajouei, G.H. Hakimelahi, D. Abedi, E. Jafari and F. Hassanzadeh, *Res Pharm Sci* 2012, **7**, 151-158
- 37 F. Hassanzadeh, E. Jafari, G.H. Hakimelahi, M.R. Khajouei, M. Jalali and G.A. Khodarahmi, *Res Pharm Sci.*, 2012, **7**, 87-94
- 38 R. Whomsley, I.E. Fernandez, P.J. Nicholls, H.J. Smith, P. Lombardi and V. Pestellin, *J Steroid Biochem Molec Biol.*, 1993, **44**, 675-6
- 39 G.A. Khodarahmi, C.A. Laughton, H.J. Smith and P.J. Nicholls, *J Enz Inhibit.*, 2001, **16**, 401-416
- 40 M.R. Saberi, T.K. Vinh, S.W. Yee, B.J.N. Griffiths, P.J. Evans and C Simons, *J Med Chem.*, 2006, **49**, 1016-1022
- 41 M.A.C. Neves, T.C.P. Dinis, G. Colombo and M.L.S. Melo, *J Med Chem.*, 2009, **52**, 143-150
- 42 N. Suvannang, C. Nantasenamat, C. Isarankura-Na-Ayudhya and V. Prachayasittikul, *Molecules.*, 2011, **16**, 3597-3617
- 43 J. Sgrignani and A. Magistrat, *J Chem Inf Mod.*, 2012, **52**, 1595-1606
- 44 R. Huey and G.M. Morris , Using AutoDock4 with AutoDockTools: A Tutorial. California: The Scripps Research Institute Molecular Graphics Laboratory. 2006
- 45 A.D. Favia, A. Cavalli, M. Masetti, A. Carotti and M. Recanatini, *Proteins*, 2006, **62**, 1074-1087
- 46 M.J. Frisch, G.W. Trucks, H.B. Schlegel, G.E. Scuseria, M.A. Robb, J.R. Cheeseman and G. Scalmani, Gaussian Development Version, Revision B.01, Gaussian. Inc., Wallingford CT. 2009
- 47 S. Dapprich, I. Komaromi, K.S. Byun, K. Morokuma and M.J. Frisch, *J Mol Struct: Theochem.*, 1999, **462**, 1-21